

Time-Resolved FTIR Spectroscopy of the Photointermediates Involved in Fast Transient H⁺ Release by Proteorhodopsin

Yaowu Xiao, Ranga Partha, Richard Krebs, and Mark Braiman*

Department of Chemistry, Syracuse University, Syracuse, New York 13244-4100

Received: August 16, 2004; In Final Form: October 8, 2004

Proteorhodopsin (pR) is a homologue of bacteriorhodopsin (bR) that has been recently discovered in oceanic bacterioplankton. Like bR, pR functions as a light-driven proton pump. As previously characterized by laser flash induced absorption spectroscopy (Krebs, R. A.; Alexiev, U.; Partha, R.; DeVita, A. M.; Braiman, M. S. *BMC Physiol.* **2002**, 2, 5), the pR photocycle shows evidence of light-induced H⁺ release on the 10–50 μ s time scale, and of substantial accumulation of the M intermediate, only at pH values above 9 and after reconstitution into phospholipid followed by extensive washing to remove detergent. We have therefore measured the time-resolved FTIR difference spectra of pR intermediates reconstituted into DMPC vesicles at pH 9.5. A mixture of K- and L-like intermediates, characterized by a 1516 cm⁻¹ positive band and a 1742 cm⁻¹ negative band respectively, appears within 20 μ s after photolysis. This mixture decays to an M-like state, with a clear band at 1756 cm⁻¹ due to protonation of Asp-97. The 50–70 μ s rise of M at pH 9.5 is similar to (but a little slower than) the rise times for M formation and H⁺ release that were reported earlier based on flash photolysis measurements of pR reconstituted into phospholipids with shorter acyl chains. We conclude that, at pH 9.5, H⁺ release occurs while Asp-97 is still protonated; i.e., this aspartic acid cannot be the H⁺ release group observed by flash photolysis under similar conditions.

Introduction

Proteorhodopsin (pR)⁴¹ is a light-activated proton pump that was recently discovered in oceanic γ -proteobacteria and that is homologous to bacteriorhodopsin (bR).^{1,2} Like bR, pR has seven trans-membrane α -helices containing several residues conserved among archaeal rhodopsin proton pumps. In particular, homologues of Asp-85, Asp-96, Arg-82, and Lys-216 in bR are also present in pR.

However, homologues of Glu-194 and Glu-204 of bR are conspicuously absent from pR.³ These two residues, along with Arg-82, are believed to be involved in the fast (\sim 50 μ s) H⁺ release step of the bR photocycle, which is normally coincident with formation of the M photoproduct.^{4–6} Flash induced absorption experiments demonstrate that, under certain conditions (pH 9.5 and in the presence of phospholipids), the absence of homologues for these two Glu residues in wild-type pR does not preclude fast H⁺ release.⁷ This suggests that fast H⁺ release by pR might involve different residue(s) than in bR, which need to be identified. Under the same conditions used to detect fast H⁺ release, an M-like photoproduct of pR, characterized by an absorption band near 410 nm, appears at room temperature with a rise time of <10 μ s after photolysis, and reaches its concentration maximum within 100 μ s. However, other workers, using different reconstitution conditions, observed a 5–10 times slower formation of M from pR, giving a maximum concentration of M around 0.5–1 ms.^{8–11}

Time-resolved Fourier transform infrared (TR-FTIR) spectroscopy has been successfully used in examining residues undergoing protonation changes during the bR photocycle.^{12–17} With this method, the positive peaks in the difference spectrum

at a given time after a photolysis pulse indicate functional groups present in the photoproduct(s) that were not in the initial unphotolyzed structure. Negative peaks are due to structures present in the starting state that are depleted upon photolysis. There is broad agreement on the frequencies, intensities, and vibrational assignments of hundreds of such peaks in TR-FTIR difference spectra that have been obtained from all of the bR photointermediates in the predominating linear sequence (bR \rightarrow J \rightarrow K \rightarrow L \rightarrow M \rightarrow N \rightarrow O \rightarrow bR).

We have now measured time-resolved FTIR difference spectra of pR intermediates under conditions that are known to support fast H⁺ release (pH 9.5, and in the presence of phospholipids). The detection of protonated Asp-97 in the M intermediate occurring on the same time scale as previously measured fast light-induced H⁺ release from pR⁷ clearly rules out this aspartic acid as the H⁺ release group. This leaves the identity of this group still undetermined. The most obvious remaining candidate is Arg-94, the homologue of Arg-82 in bR that time-resolved FTIR studies indicate as undergoing a nearly stoichiometric deprotonation upon M formation in bR.¹⁸

Additionally, we report here the first vibrational spectral features assignable to an L-like photoproduct of pR, in the form of a negative band at 1742 cm⁻¹ in FTIR difference spectra measured 20–90 μ s after photolysis in the presence of phospholipid at pH 9.5. This L-like feature in the difference spectrum overlaps with the lifetime of K and has not yet been kinetically separated, suggesting that there may be an L \rightarrow K back reaction leading to a rapid equilibration of these two species. Both K-like and L-like species appear to decay together to form the M-like intermediate with a time constant of 50–70 μ s at 22 °C, confirming the rise time of M that was measured using UV/vis flash photolysis under conditions of pH 9.5 and phospholipid reconstitution.⁷

* Corresponding author. Telephone: (315) 443-4070. Fax: (315) 443-4070. E-mail: mbraiman@syr.edu.

Experimental Procedure

Sample Preparation. Purified pR solubilized in octyl- β -D-glucoside (OG) was obtained using previously published procedures.^{1,7} Both wild-type pR and the triple cysteine mutant (TCM) were expressed and prepared similarly. In brief, pR was isolated from *E. coli* (strain UT5600), transformed with a plasmid encoding the pR gene with an Ara promoter and ampicillin resistance. This expression plasmid includes a region coding for a C-terminal His₆ tag that can be used for Ni²⁺-column purification, but such a procedure was not used here. Instead, the membrane pellet was solubilized in OG, and then this detergent extract was purified using Phenylsepharose and hydroxylapatite columns. The purified pR samples were reconstituted into 1% 1,2-dimyristoyl-*sn*-glycero-3-phosphocholine (DMPC) vesicles. This was done as follows. The pR in 1% OG was gently mixed with the DMPC lipid, presolubilized in 1% OG at a 1:2 lipid:detergent ratio; then the mixture was concentrated \sim 30-fold using Vivaspinn 20 centrifugal concentrators (Vivascience Inc.) at 3500g and 4 °C; then the original sample volume was restored with fresh detergent-free buffer (10 mM Tris-Cl, pH 9.5); this concentration/washing step was repeated a minimum of three more times to remove octylglucoside thoroughly, before pelleting the resulting pR-containing vesicles in a microcentrifuge tube at 3500g.

To prepare protein samples for IR spectroscopy, the pR-containing vesicles were washed twice additionally in 10 mM Tris-Cl buffer of appropriate pH value, and then centrifuged at 2000g and 4 °C for 1 h to pellet the membranes. The pellet was partially air-dried; then a \sim 1 μ L portion of it was compressed to \sim 5–10 μ m thickness between two CaF₂ windows, sealed with vacuum grease around the sample perimeter. The relative H₂O content (w/w) in the samples is estimated to have been 40–60%, based on an observed ratio of $A_{1650}/A_{1550} = 1.5 \pm 0.2$ in the static IR spectrum.¹³

FTIR Spectroscopy. A Nicolet Magna-IR860 spectrometer (Thermo Nicolet Instrument Corporation, Madison, WI) was utilized in step-scan time-resolved mode. Its 20-MHz photovoltaic HgCdTe detector is equipped with dual ac- and dc-coupled outputs. The dc output represents the absolute IR intensity reaching the detector, while the ac output represents the transient changes in intensity. Low-pass and high-pass electronic bandwidth filters, with $\nu_{1/2} = 11\,000$ Hz and $\nu_{1/2} = 200$ Hz, respectively, were applied to the detector signal in order to improve the signal-to-noise ratio. A pulsed frequency doubled Nd³⁺:YAG laser (532 nm, 10 mJ cm⁻²) was used to initiate the photocycle. The interval between successive laser flashes was 1.5 s. A long-pass optical filter with 5- μ m cutoff was placed in the IR beam between the sample and detector, to block scattered light from the Nd³⁺:YAG laser and to limit the optical bandwidth.

The OMNIC software (furnished along with the spectrometer by the manufacturer) was set to measure differential interferograms covering 280 μ s before to 1720 μ s after photolysis in 20 μ s increments. Spectral resolution was 8 cm⁻¹. The difference interferograms were apodized and Fourier transformed, and then phase-corrected using the phase array calculated from the dc-coupled reference interferogram. The latter was collected by the OMNIC time-resolved software, by digitizing the dc-coupled output from the detector (simultaneously with the ac-coupled output). The series of intensity difference spectra were then converted to absorbance difference spectra, by using the preflash static spectrum as background, as described previously.⁶

Results

Time-Resolved FTIR Spectra. Figure 1 shows time-averaged absorbance difference spectra measured at a broad range

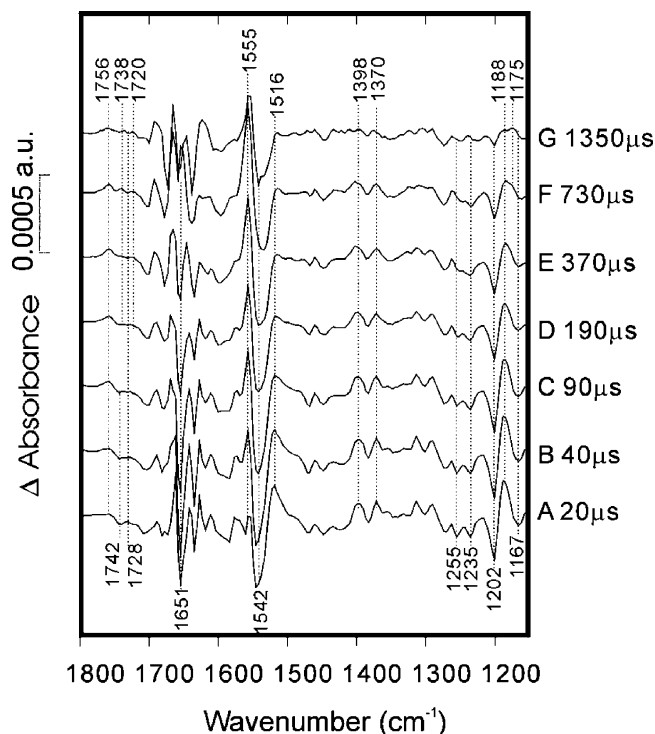


Figure 1. Time-resolved FTIR difference spectra of pR in pH 9.5 buffer solution at room temperature. Spectra taken originally at linearly spaced intervals of 20 μ s were group averaged with a quasi-logarithmic time base. Each indicated time represents the center of an averaged range. Spectral resolution is 8 cm⁻¹. The same ordinate scale is used for spectra B–G, with a fixed offset between them for clarity. To provide a first-order correction for the instrumental rise time of 15 μ s, spectrum A was rescaled by a factor of 1.4.

of times following photolysis, and Figures 2 and 3 show more detailed temporal behavior from the same data set over limited time ranges. In their most prominent features, the spectra are similar to pR photoproduct difference spectra recorded previously.^{8,9,19}

The strongest band in absolute magnitude corresponds to a negative peak near 1542 cm⁻¹. This negative band is most likely due to the C=C double bond of retinal in the unphotolyzed state. However, the precise wavenumber value of the band minimum progressively downshifts from 1546 cm⁻¹ in the 20 μ s spectrum to 1539 cm⁻¹ in the 1350 μ s spectrum (Figure 1). This is likely due to spectral overlap with time-varying positive $\nu_{C=C}$ bands, corresponding to 1516 and 1555 cm⁻¹ in photoproducts that predominate at earlier and later times, respectively.

The C–C single bond stretches of the retinylidene chromophore generally absorb in the fingerprint region between 1150 and 1280 cm⁻¹. The strong negative IR bands at 1167 and 1202 cm⁻¹ are consistent with a pR starting structure containing an all-*trans*-retinylidene protonated Schiff base. In agreement with earlier conclusions,^{3,8,19} we find no evidence for substantial amounts of a parallel photocycle starting with the 13-*cis* configuration of the retinylidene chromophore. In none of the spectra in Figure 1 is there a negative band near 1185 cm⁻¹ that would indicate contributions from such a photocycle. This observation is somewhat surprising, given that 13-*cis* chromophore is likely to be present at a level as high as 40% in our starting state, based on recently published chromophore extraction measurements of pR.⁹

The negative band at 1651 cm⁻¹ in Figure 1 can be assigned to $\nu_{C=N}$ of the protonated Schiff base in the unphotolyzed state of pR, based on Raman studies showing the downshift of a band

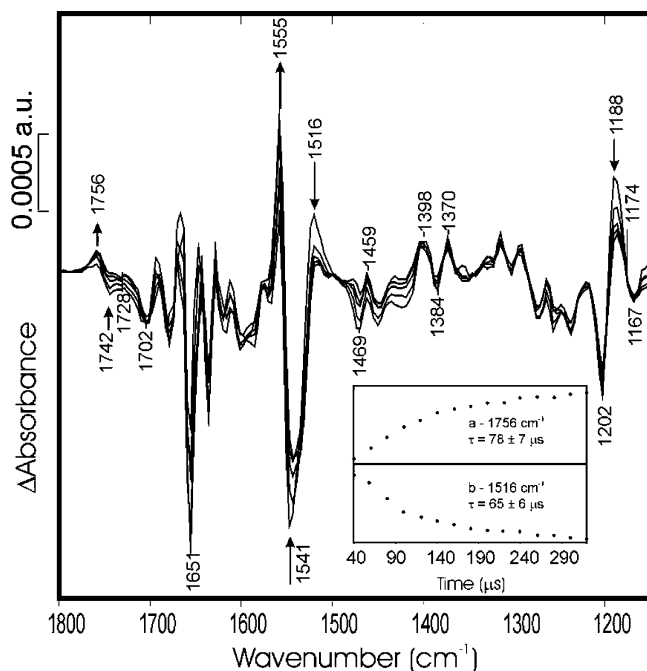


Figure 2. FTIR difference spectra of pR at 40, 100, 160, 220, and 280 μs after photolysis are shown directly overlaid. These are individual time-slice spectra from the same data set used to calculate the averaged spectra in Figure 1. Arrows represent relative values of dA/dt at different band positions. Inset: lines are single-exponential fits of the absorbance changes at (a) 1756 and (b) 1516 cm^{-1} , with experimental data indicated by the dots.

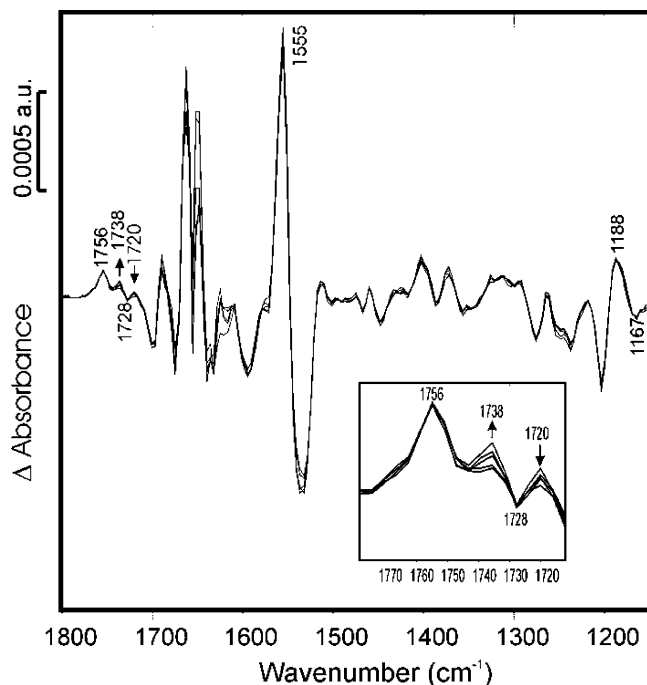


Figure 3. Individual time slices of FTIR difference spectra of pR observed at 520, 540, 560, 580, and 600 μs after photolysis are shown directly overlaid. The spectra are from the same data set used to calculate the averaged spectra in Figure 1. Arrows represent relative values of dA/dt at different band positions. Inset: enlarged spectral range 1700–1780 cm^{-1} , showing the shift in intensity from 1720 to 1738 cm^{-1} .

near this frequency when pR is suspended in $^2\text{H}_2\text{O}$ or reconstituted with $15\text{-}^2\text{H}$ -retinal.^{3,9} In fact, resonance Raman spectra obtained with green excitation wavelengths³ show a splitting of the band assigned to $\nu_{\text{C}=\text{N}}$, with overlapping components

centered at 1642 and 1656 cm^{-1} . This splitting is not observed in the FTIR spectrum at pH 9.5 in Figure 1, probably due to the limited (8 cm^{-1}) resolution of the time-resolved IR measurements, as compared to 6 cm^{-1} for the Raman spectra.³ The observed single band at 1651 cm^{-1} in Figure 1 likely represents the superposition of the unresolved $\nu_{\text{C}=\text{N}}$ frequencies, perhaps along with an overlapping negative amide I difference band. The 1651 cm^{-1} frequency is 13 cm^{-1} lower than the most recently reported value for $\nu_{\text{C}=\text{N}}$ in low-temperature FTIR difference spectra,¹⁹ but the reason for this difference is unclear.

The most important observations in Figure 1 relate to the bands above 1700 cm^{-1} , which are mainly due to the C=O stretch vibrations of protonated carboxylic acids. The largest band, at 1756 cm^{-1} , is reminiscent of the 1754–1762 cm^{-1} bands caused by protonation of Asp-85 in the M, N, and O states of bR. Indeed, the 1756 cm^{-1} band in FTIR spectra of pR has already been assigned to Asp-97 based on comparisons of the 5 $^\circ\text{C}$ static FTIR difference spectra of wild-type pR and the D97E mutant.⁸

In addition to a negative band at 1728 cm^{-1} on a time scale from 370 to 1350 μs (Figure 1E–G), we also observe a weaker negative band at 1742 cm^{-1} at earlier times (Figure 1A–C). The presence of the small 1742 cm^{-1} negative peak in the spectra recorded before 100 μs was not observed in previous TR-FTIR spectra of pR.^{8,9}

Equilibrium of K- and L-like Intermediates. The 20 μs spectrum in Figure 1 was rescaled to normalize the size of the negative band at 1167 cm^{-1} to its value in the 90 μs spectrum. This normalization, by a factor of 1.4, is appropriate to correct for the instrumental rise time that arises from the 11-kHz low-pass filter applied to the IR detector's analog signal before digitization. The biggest effect of the resulting 15 μs instrumental time constant ($2\pi \times 11 \text{ kHz}$)⁻¹ is to suppress the amplitude of all the difference bands collected during the earliest time slices after photolysis. The difference spectra at delay times of 40 μs and later were essentially unaffected by this instrumental time constant, as verified by the constant (and eventually decreasing) magnitude of the negative band at 1167 cm^{-1} .

The spectra at earlier times ($<100 \mu\text{s}$) in Figure 1A–C are similar in most features to a previously published 14 μs spectrum of pR photoproducts at pH 8.5⁹ and to the recently published pR \rightarrow K spectrum obtained from low-temperature experiments.¹⁹ Specifically, as with the earlier measurements, our data (Figure 1A–C) show negative bands at 1255, 1235, 1202, and 1167 cm^{-1} as well as large positive bands near 1188 and 1516 cm^{-1} . Of these, only the 1235 cm^{-1} band is not observed in bR photoproduct difference spectra.⁹

From the well-established correlation between the ethylenic band frequency and the absorption maximum of retinal pigments,²⁰ the positive band observed at 1516 cm^{-1} in Figure 1A–C corresponds to an expected λ_{max} value of $\sim 600 \text{ nm}$, meaning that the predominant photoproduct on this time scale corresponds to a state resembling the K photoproduct of bR. A similar conclusion was reached by other workers.^{8–10}

Nevertheless, a new 1742 cm^{-1} negative band is present in the earlier spectra over the 20–90 μs time range (Figure 1A–C). This band appears within 20 μs at pH 9.5 (Figure 1A), the time resolution of our measurements. It is more easily observed at later times in spectra under progressively less basic conditions, down to an estimated pH near 8 (see Figure 4). This band indicates the presence of another intermediate over the 20–90 μs time scale at pH 9.5, which bears some similarities to the L state of bR. Such an L-like intermediate of pR was not previously reported at pH 9.5 with TR-FTIR^{8,9} or UV/vis

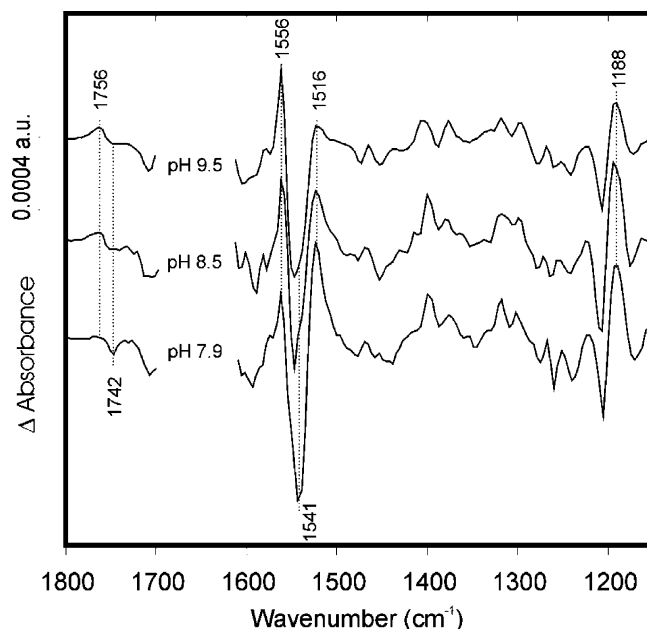


Figure 4. Time-averaged FTIR spectra of pR covering the time range 50–200 μ s at different pH values. The spectra have been scaled by the size of the negative band at 1541 cm^{-1} . The spectral region 1700–1600 cm^{-1} was blanked due to the poor signal-to-noise ratio in this region. pH values are given for the buffer that was present before partial air-drying.

spectroscopy.^{10,11,21} However, in all of these reports nonionic detergents (lauryl maltoside or octylglucoside) were used during sample preparation, and in none of them were procedures employed to thoroughly remove the detergent.

Formation of M Intermediate. To visualize the small spectral changes at later times, our 40, 100, 160, 220, and 280 μ s FTIR difference spectra at pH 9.5 are shown directly overlapped in Figure 2. The perfect overlap of the bands at, for example, 1167 cm^{-1} in all five spectra indicates the accuracy and high signal-to-noise ratio. This band is expected to remain constant during the evolution of the photoproduct states, because for pR as for bR, its intensity probably corresponds exclusively to the depletion of the all-*trans*-retinal chromophore. Also, the almost complete overlap of the bands at 1398 and 1702 cm^{-1} , and the near-perfect isosbestic point near 1174 cm^{-1} , indicate the high signal-to-noise ratio of these spectra.

In Figure 2 six bands, at 1756, 1742, 1555, 1541, 1516, and 1188, and cm^{-1} , are marked with arrows in order to represent their temporal evolution. The relative sizes and directions of these correspond to intensity changes at these frequencies over the time range 40–280 μ s. These bands are likely associated with conversion of the K/L mixture to M. The simple time-dependent behaviors of two important vibrational difference bands, at 1756 and 1516 cm^{-1} , are plotted in the inset.

The intensity change of the positive band at 1756 cm^{-1} fits well to a single-exponential curve with a rise time of 78 ± 7 μ s, as shown in the Figure 2 inset. In the bR photocycle, a positive band around 1760 cm^{-1} is due to the C=O stretch of Asp-85. For bR, the intensity increase at 1760 cm^{-1} is specific for M formation; later photoproducts (N, O) have somewhat lower $\nu_{\text{C=O}}$ frequencies. The positive band at 1756 cm^{-1} in Figure 2 is assigned to the C=O stretch of protonated Asp-97 in pR, similar to the 1755 cm^{-1} band previously reported for pR photointermediates.^{8,9} Appearance of this band provides the best indicator in the IR spectral range for formation of an M-like intermediate in the pR photocycle.

The positive band at 1516 cm^{-1} is assignable to the most intense C=C stretch mode of the K-like intermediate formed. This band shows a high intensity in the K-like pR photoproduct spectra (Figure 1A–C), but is significantly reduced in the M-like pR spectra (Figure 1D–G). This indicates that the decay of the 1516 cm^{-1} band in Figure 2 corresponds to the decay of the K-like intermediate. This decay also fits a single-exponential curve with a time constant of about 65 μ s (shown in the inset of Figure 2). This value is similar to the time constant of M-like photoproduct formation measured at 1756 cm^{-1} , suggesting the possibility of a direct K \rightarrow M conversion.

However, the additional negative band at 1742 cm^{-1} in Figure 2 contradicts such a conclusion, by indicating the presence of an L intermediate. The signal-to-noise ratio at this frequency was, however, not adequate to determine accurately the time constants for this band. From Figure 4, the time constant of L decay strongly depends on pH. More specifically, L decay and M formation are significantly slowed at a lower pH and thus the L intermediate is more easily observed. In other words, in the pR photocycle, the second step in the sequential model K \rightarrow L \rightarrow M is greatly accelerated by a pH rise. Therefore, it can be expected that the inability to observe any L intermediate in previous time-resolved UV/vis or FTIR spectroscopy (using different reconstitution conditions) is most likely due to kinetic reasons, as proposed previously,^{8,10} rather than to the true absence of an L intermediate. Our proposed K \rightarrow L \rightarrow M sequential reaction, however, does not necessarily exclude the possibility of a parallel direct K \rightarrow M conversion. From the two time constants for the 1756 and 1516 cm^{-1} bands, we conclude that the time constant for the K/L \rightarrow M conversion in pR reconstituted in DMPC at pH 9.5 and room temperature is ~ 70 μ s.

Perturbation of a Carboxylic Group. Two small positive bands at 1720 and 1738 cm^{-1} can be discerned in the 730 and 1350 μ s spectra (Figure 1F,G). Additionally, a small negative band at 1728 cm^{-1} appears contemporaneously with the two positive bands. To observe the evolution of these bands before 730 μ s, our FTIR difference spectra in the range 520–600 μ s are shown directly overlapped in Figure 3. This range was limited to times < 600 μ s, to reduce the effects of the ~ 800 μ s time constant of the ac-coupled detector. No normalization was performed. The perfect overlap of the bands at 1167, 1188, and 1756 cm^{-1} in all five spectra indicates a high signal-to-noise ratio and constant baseline. The constant intensities of the 1188 and 1756 cm^{-1} bands in the time range 520–600 μ s suggest that the M photoproduct and its precursor(s) have reached an equilibrium.

From Figure 3, the positive 1720 cm^{-1} band appears to shift in intensity to 1738 cm^{-1} over time. Both positive bands appear to be paired with the same negative band at 1728 cm^{-1} . The 1720(+)/1728(–) pair likely corresponds to the 1717(+)/1728(–) pair in the previously observed 1-ms difference spectrum of pR at pH 8.5.⁹ It is not clear whether the other 1738(+)/1728(–) pair corresponds to the 1742(+)/1728(–) pair observed by Dioumaev et al.,⁸ because the time scales for appearance of the respective pairs are quite different. The pairing of the negative 1728 cm^{-1} band in Figure 3 with respective positive bands in a nearby spectral region, as well as their much smaller size compared with the 1756 cm^{-1} band, strongly suggests an environmental perturbation of a protonated carboxylic group, rather than a change in protonation state.

Global Multiexponential Fit. The time-resolved FTIR difference spectra (as in Figure 1), covering a time range 40–1720 μ s, were fitted by using the “FITEXP” program.^{22,23} The

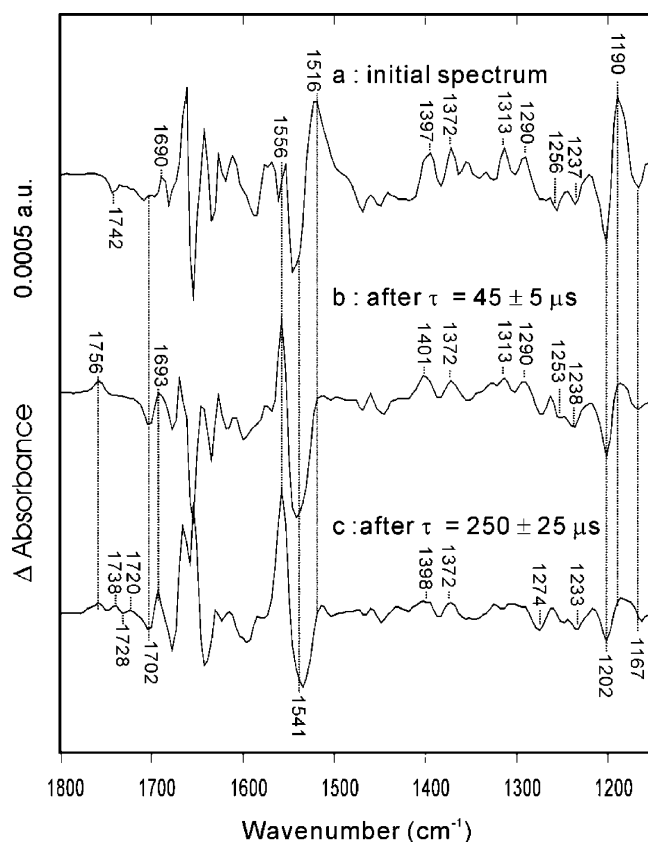


Figure 5. Calculated time-resolved difference spectra of pR and its photoproducts, based on a global least-squares multiexponential fit to the difference spectra in Figure 1. (a) The pR \rightarrow K/L mixture difference spectrum, obtained as the initial spectrum from a global analysis of the pR photocycle over the time range 40–1720 μ s at 22 $^{\circ}$ C. (b) Calculated pR \rightarrow M difference spectrum, obtained from the fastest-decaying amplitude spectrum (K/L mixture \rightarrow M) plus the corresponding initial spectrum (pR \rightarrow K/L of Figure 5a). (c) Calculated pR \rightarrow perturbed-M difference spectrum, obtained from the second-fastest-decaying amplitude spectrum (M \rightarrow perturbed M) plus the corresponding calculated M spectrum (pR \rightarrow M of (b)).

first 20- μ s spectrum was not included in the fit because its amplitude is heavily affected by the \sim 15 μ s time constant of the low-pass electronic filter on the ac-coupled detector. Assuming this truncated photocycle, three exponentially decaying spectra plus a constant-amplitude spectrum were needed to fit the spectra in Figure 1. The first two fitted time constants are 45 ± 5 and 250 ± 25 μ s, whereas the last one is around 1 ms, close to the \sim 800 μ s time constant of the high-pass electronic filter on the ac-coupled detector. The spectra obtained by the analysis may thus be distorted for the last intermediate, because of the truncated description of the photocycle and/or effects from the electronic filter. The earlier spectra, however, should not be influenced by the limited data acquisition period.

The initial spectrum, shown in Figure 5a, corresponds to the difference spectrum of the pR \rightarrow K/L mixture. This is indicated by the negative band at 1742 cm^{-1} characteristic of a carboxylic acid group, by a large positive band at 1516 cm^{-1} due to the retinal C=C stretch mode in K, and by a relatively large positive band at 1188 cm^{-1} due to a chromophore vibration of the 13-*cis*-retinylidene protonated Schiff base present in K and L.

The first time-dependent amplitude spectrum obtained from the "FITEXP" program has a \sim 50 μ s decay time, in general agreement with the value determined for the K/L \rightarrow M conversion based on band evolutions at 1756 and 1516 cm^{-1} (Figure 2), and is therefore likely to correspond to a K/L \rightarrow M

difference spectrum. By adding to this the pR \rightarrow K/L difference spectrum (corresponding to the initial spectrum from the global fit), it is possible to obtain a difference spectrum that (in theory) corresponds to the pR \rightarrow M difference spectrum, as shown in Figure 5b. The features of this spectrum are generally close to those of the pure pR \rightarrow M difference spectrum measured from the E108Q mutant,⁸ although a small 1188 cm^{-1} positive band above the baseline may indicate some contributions from non-M impurities.⁹ The positive band at 1693 cm^{-1} , paired with a negative band at 1702 cm^{-1} , has recently been assigned to perturbed Asn-230 in M.¹⁹ In addition, an almost complete disappearance of the negative band at 1702 cm^{-1} in the N230A mutant pR \rightarrow M difference spectrum indicates that no major part of this band could be assigned to any carboxylic acid group, such as Asp-227, acting as a H⁺ release group during the pR \rightarrow M reaction.

It is notable that the positive band at 1556 cm^{-1} in Figure 5b is much sharper, and greater in maximum relative intensity, than the corresponding bands in the L, M, or N intermediates of bR. This was also previously observed in pR \rightarrow M FTIR difference spectra of the E108Q pR mutant,⁸ but not in the pR \rightarrow M difference spectrum obtained at cryogenic temperature.¹⁹ A much stronger positive band around 1556 cm^{-1} in bR \rightarrow M difference spectra has consistently been observed at room temperature than at cryogenic temperature.^{24,25} Part of the intensity of this band has very recently been assigned to Arg-82, indicating its nearly stoichiometric deprotonation in the M state of bR.¹⁸

Figure 5c was obtained by adding the relatively pure pR \rightarrow M difference spectrum of Figure 5b to the second time-dependent amplitude spectrum from the "FITEXP" program. This calculated spectrum clearly shows perturbations of a carboxylic acid, as evidenced by the 1738(+), 1728(-), and 1720(+) bands. The first two are reminiscent of the band pair at 1740(+)/1732(-) in the bR \rightarrow M difference spectrum, indicating an environmental perturbation of Asp-115 in the M state.²⁶ However, this residue is not conserved in pR. On the other hand, the 1738, 1728, and/or 1720 cm^{-1} bands could belong to an intermediate after M, e.g., N, as indicated by the strong positive band at 1555 cm^{-1} in Figure 5c.

Global fitting results of the TR-FTIR spectra from the TCM reconstituted with the same method as the wild-type pR are shown in Figure 6. Most of the spectral features in Figure 5 are reproduced in Figure 6. In particular, the 1742 cm^{-1} negative band and 1516 cm^{-1} positive band indicate a K/L mixture (Figure 6a) is the precursor for M, which shows a characteristic 1756 cm^{-1} positive band (Figure 6b). More importantly, the triple mutant shows similar photocycle kinetics as wild-type, confirming results from Dioumaev et al.²¹ that this mutant resembles the wild type. However, our results on both the wild type and the TCM remain in disagreement with the results of Dioumaev et al., with regard to the time scale of M formation and the observability of an L-like precursor to M.

Discussion

The goal of this study was to analyze spectroscopically the photointermediates of the pR photocycle under the unique conditions where fast H⁺ release has previously been measured to occur.⁷ Therefore, we reconstituted pR in DMPC vesicles at pH 9.5 and measured its spectra using a time-resolved FTIR spectrometer. By contrast, all previous FTIR measurements were performed using different sample conditions where H⁺ release did not accompany M formation. In one case, this was due to the use of a lower pH of 8.5,⁹ under which conditions it is now known that fast H⁺ release is blocked.⁷

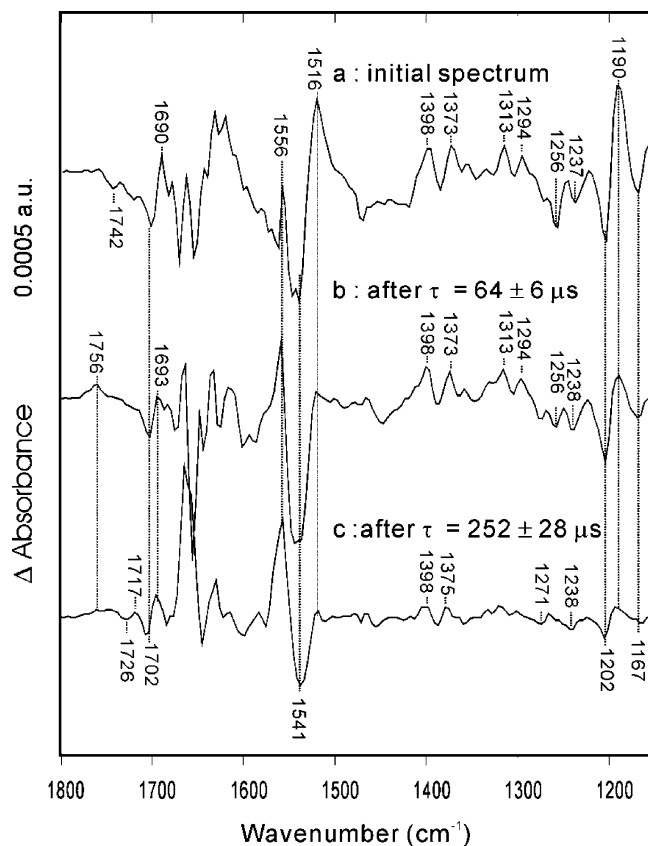


Figure 6. Calculated time-resolved difference spectra of pR triple cysteine mutant and its photoproducts. FTIR sample preparation, TR-FTIR measurements, and kinetic fitting of the TR-FTIR spectra are identical to those of wild-type pR.

In the other case,⁸ the key difference in sample preparation may be that nonionic detergent was not adequately removed during sample preparation. The other workers treated their samples during purification with lauryl maltoside, which has a critical micelle concentration (cmc) of about 0.01% (w/w).²⁷ By contrast, the OG used in our work has a cmc above 0.5%,²⁸ i.e., 50-fold greater. No procedures were described in the work of Dioumaev et al.⁸ that could have reduced the lauryl maltoside concentration in their FTIR samples to below its cmc, whereas our FTIR samples reconstituted from 1% octylglucoside solution were dialyzed for 4–5 days, followed by a minimum of 3–4 pelleting/washing cycles.

Photocycle of pR within a Time Range of 20–1000 μ s.

Our analysis of the pR photocycle is dependent on comparisons with the much more extensively studied photocycle of bR. The latter has been characterized to have at least six structurally distinct photointermediate states: bR, K, L, M, N, and O. Upon absorption of a photon to form the excited-state bR*, the chromophore undergoes a rapid trans-to-cis isomerization about the C₁₃=C₁₄ double bond to form K, a red-shifted intermediate with absorption at 610 nm. The K \rightarrow L conversion is a relaxation process in which energy stored in the distorted chromophore is transferred to the protein.²⁹ At room temperature, the time scales of the bR* \rightarrow K and K \rightarrow L conversions are in the range of 10 ps and 1 μ s, respectively. The subsequent L \rightarrow M transition in bR is characterized by the deprotonation of the Schiff base to Asp-85 and by the so-called fast H⁺ release. The latter signifies the ejection of a proton from the H⁺ release group into the external medium, on the time scale of 10–100 μ s at room temperature depending on pH and reconstitution conditions. The identity of the proton release group in bR is still controversial,

but direct evidence from time-resolved vibrational spectroscopy points most firmly to Arg-82¹⁸ and/or an H₂O₂⁺ ion.³⁰

Time-resolved UV/vis spectroscopy and FTIR spectroscopy have recently been applied to pR.^{7–11,21,31} The resulting photocycle observations depend strongly on the pH used for the measurements. At pH 5, i.e., 2–3 pH units lower than the pK_a of Asp-97, a red-shifted K state as well as a subsequent L-like intermediate are detected in kinetically fitted spectra, but no M intermediate has been detected.^{11,21,31} At pH 9.5, global analysis of the time-resolved UV/vis and FTIR spectra predicted the existence of at least six intermediates,^{8,9} including K, M, N, and O. A multiphasic K \rightarrow M conversion occurs throughout \sim 1 ms after photolysis, with two to three distinct exponential time constants, but the intervening L intermediate cannot be observed. Our results support the conclusion that this was not because L is never formed, but instead is most likely due to the kinetic reasons proposed by the authors.^{8,10}

Our time-resolved FTIR spectra of pR under fast H⁺ release conditions (pH 9.5 and a detergent-free phospholipid environment) show that, when measured at a time resolution of 20 μ s, K decays to L and/or M intermediates with only one time constant of 50–70 μ s. This value is much slower than that for bR, but is faster than the slowest component of the multiphasic K decay proposed earlier for pR, and therefore indicates a shorter lifetime of K compared to the value of \sim 1 ms reported by others.^{8–10,21} More specifically, our current TR-FTIR measurements indicate that K is mostly depleted within 100 μ s, and shows almost no presence in the 400 μ s spectrum, as measured by the magnitude of the 1516 cm^{−1} band (Figure 1). As a result of the faster K decay in our measurements, M accumulates faster, and in fact clearly predominates at delays $>$ 200 μ s. In contrast, a much lower concentration of M in the same time range has been reported by others.^{8–10,21}

Our time-resolved FTIR measurements of pR indicate that when sample preparation conditions include the use of pH 9.5, as well as rigorous removal of nonionic detergent following phospholipid reconstitution, the L intermediate can be accumulated to a concentration high enough to be detected. L was reported by others as undetectable even at pH 9.5, but this is most likely due to the use of different sample preparation methods, as noted above. Our UV/vis and TR-FTIR results in combination suggest that fast H⁺ release, formation of M on the \sim 50 μ s time scale, and buildup of substantial concentrations of the L intermediate are all only detectable from the pR sample with a purity $>$ 90% and with homogeneous phospholipid reconstitution followed by a rigorous removal of detergent, involving sufficient washing and/or dialysis to bring the detergent concentration to below the cmc. Even this description may represent only necessary, but not always sufficient, conditions for obtaining results such as shown in Figures 5 and 6. So far, when we have attempted to replace the Phenyl-sepharose/hydroxylapatite procedures described under Experimental Procedure with citrate precipitation and/or affinity chromatography using an Ni²⁺–NTA column, the resulting pR samples showed much smaller IR difference spectra, with little or no M intermediate formation (data not shown).

In our FTIR samples, the K/L \rightarrow M conversion has a phenomenological time constant of about 50–70 μ s, a bit slower than the \sim 10 μ s time constant reported earlier based on 410 nm absorption changes.⁷ We attribute this difference to the use of different phospholipids. In the current FTIR experiments, we use DMPC rather than DHPC in order to simplify the preparation of partially dried samples and to improve its stability upon repeated laser irradiation. In the previous UV/vis absorption

experiments, on the other hand, the short-chain phospholipid DHPC was utilized to avoid light scattering artifacts. An alternative explanation for the slower time constant measured in the current work is that FTIR measurements were carried out in concentrated samples with only ~50% water by weight, whereas the laser-induced absorbance spectra⁷ were obtained on a suspension or a solution of pR in short-chain lipid. The higher extent of hydration used in UV/vis measurements might have promoted more rapid M formation and H⁺ release. In the bR photocycle, the rate of K → L conversion is strongly affected by hydration.³² Similarly, in the pR photocycle under basic conditions, a decrease in sample humidity has been demonstrated to cause a significantly slowed photocycle.¹¹

Assignment of Glu-108 Frequency in Unphotolyzed pR. In bR, a negative band at 1742 cm⁻¹ in the bR → N difference spectrum signals deprotonation of Asp-96. However, additionally in the bR → L difference spectrum, an even larger negative band around 1742 cm⁻¹ is observed. This band was also assigned largely to $\nu_{\text{C=O}}$ of Asp-96 in unphotolyzed bR, with the conclusion that this residue is perturbed and/or partially deprotonated in L.^{33,34} Therefore, on the 1–50 μs time scale, appearance of the 1742 cm⁻¹ negative band is typically used as an indicator for L, and its subsequent intensity decrease can be used to measure the rate of L decay to M.³³

By analogy, appearance of the 1742 cm⁻¹ negative band in Figure 1A–C suggests that the homologous glutamic acid (Glu-108) in pR undergoes an environmental change (and/or deprotonation) upon formation of the K/L mixture. The 1742 cm⁻¹ negative band that we observe on the time scale of 20–90 μs (Figure 1A–C) is identical in frequency to the band observed for the Asp-96 $\nu_{\text{C=O}}$ in bR → L and bR → N difference spectra. However, such an assignment would appear to contradict the previously published assignment of a negative band at 1727 cm⁻¹ to $\nu_{\text{C=O}}$ of protonated Glu-108 in unphotolyzed pR.^{8,9} In particular, in difference spectra measured at ≥ 10 ms, wild-type pR shows a 1727(–)/1742(+) pair; in the E108D mutant this pair apparently upshifts to 1744(–)/1757(+).⁸ In another study,⁹ a 1-ms difference spectrum of pR at pH 8.5 was obtained and a negative FTIR band at 1728 cm⁻¹ was assigned to Glu-108, on the basis of an expectation for deprotonation of Glu-108 on the time scale where the 1728 cm⁻¹ negative band is observed.

We also observe a negative 1728 cm⁻¹ band on the time scale expected for N (or perturbed M) formation (e.g., Figure 3 inset). However, rather than a single corresponding positive band in the spectral range of 1700–1800 cm⁻¹, we observe two, at 1720 and 1738 cm⁻¹, at different times within the 370–1350 μs range (Figure 1E–G). These two band pairs likely correspond to, but appear much earlier than, the band pairs observed previously.^{8,9} The observed positive band shift in intensity from 1720 to 1738 cm⁻¹ (Figure 1E–G and Figure 3) might well reflect the evolution of an environmental perturbation of Glu-108 after initial M formation.

If both negative bands at 1742 and 1728 cm⁻¹ could be assigned to Glu-108 in unphotolyzed states, this would indicate that our FTIR sample contains a mixture of two pR forms. That is, Figure 1 must reflect photocycles coming from two different initial states, one with Glu-108 absorbing at 1742 cm⁻¹ and the other with Glu-108 absorbing at 1728 cm⁻¹. These two states could possibly correspond to the doublet band seen in an SDS–PAGE analysis of purified pR by Krebs et al.;⁷ they might also account for the split $\nu_{\text{C=O}}$ bands attributable to the observed heterogeneous environments for Schiff base.³ The third possibility that cannot be completely excluded is that the two states

simply correspond to acidic and basic forms of pR, with Asp-97 protonated or deprotonated, respectively.

In the light-induced FTIR difference spectra of pR at pH 2.3, a negative band at ~1742 cm⁻¹ is assignable to Asp-227, based on D227N mutation studies.³⁵ However, assignment of the negative 1742 cm⁻¹ band in Figure 1A–C to an Asp-227 COOH perturbation seems unlikely, because the pK_a of Asp-227 was measured to be much lower than 7,³⁵ meaning that it should already be nearly 100% deprotonated in the unphotolyzed state of our sample at pH 9.5.

Mutated pR samples measured under reconstitution conditions similar to those we used for the wild type will ultimately be required to unambiguously assign the negative bands at 1742 cm⁻¹ (Figure 1A–C) and 1728 cm⁻¹ (Figure 1F–G).

Proton Transfers during Formation of the M State. It was previously shown that, even in the pH range 7–8.5 where fast H⁺ release is not observable, the M state of pR can be formed.^{8,9} This suggests that formation of an M-like state is necessary, but not by itself sufficient, to trigger fast H⁺ release. The same has been seen in bR. For example, bR shows M formation without fast H⁺ release in the pH range ~4–5.5.³⁶ Another example is the D85E mutant, in which the L → M formation is accelerated by a factor of 10, whereas the H⁺ release process is delayed by a factor of 2 with respect to wild-type bR.^{37,38} It is thus rationalized that fast H⁺ release of pR at pH 9.5 may be related to a specific structure separate from Asp-97—namely the H⁺ release complex—in M (and possibly L as well). During formation of these intermediates, structural changes of the H⁺ release complex presumably reduce its H⁺ affinity, but H⁺ release can also be blocked by a sufficiently low external pH that keeps the complex protonated.

The current experiments place some experimental constraints on the possible identity of the H⁺ release group in pR. It was previously suggested that Asp-97 in pR (which lacks a carboxylic residue homologous to E204 of bR) functions directly as its H⁺ release group.⁷ Similarly, in the E204Q mutant of bR, which like pR undergoes fast H⁺ release only at pH > 9, Asp-85 was suggested to serve as the H⁺ release group.³⁹ However, FTIR difference spectra of pR on the 90–1350 μs time scale after photolysis at pH 9.5 clearly show a positive band at 1756 cm⁻¹ (Figures 1–5), which is assigned to Asp-97 based on analogies to bR → M spectra and on sensitivity of this band to the D97E mutation.⁸ Fast H⁺ release in pR occurs on the same time scale as the rise of this band at pH 9.5,⁷ and in fact much before its decay. This indicates that Asp-97, the analogue of Asp-85 in bR, remains protonated well past the time scale of proton release, i.e., cannot serve as the H⁺ donor during fast proton release in pR at high pH.

It is currently impossible to identify unambiguously the H⁺ donors for fast H⁺ release in pR and bR from FTIR spectra. The H⁺ release group in bR is thought to involve (or interact strongly with) Arg-82 and several nearby residues, as well as some water molecules.^{18,30,40} Arg-82 and Tyr-83 of bR are conserved in pR as Arg-94 and Tyr-95; these two conserved residues, as well as water molecules, could therefore play homologous proton-donating roles in pR as in bR. However, there is strong evidence that the two proteins' H⁺ release complexes are structurally dissimilar in important ways, at least prior to photolysis. The C=N stretch vibration of the Schiff base in pR has a frequency near 1650 cm⁻¹ (Figure 1 and ref 3), which is significantly upshifted from the 1639 cm⁻¹ frequency seen in bR. This indicates a significant alteration of the Schiff base counterion environment in pR, compared to bR. Even more important evidence for different prephotolysis

structures of the two proteins' H^+ release complexes is the ~ 5 -unit upshift in the pK_a of Asp-97 in pR,^{8,9} from the value of 2.5 for its homologue Asp-85 in bR. The upshifted pK_a in pR shows little sensitivity to Arg-94 mutation, or to subsequent chemical treatment of this mutant with guanidinium compounds (Partha et al., submitted). These differences from bR are most easily explained by a significantly greater physical separation between Arg-94 and Asp-97 in pR, in comparison to Arg-82 and Asp-85 in bR.

Conclusion

Under conditions associated with fast ($< 50 \mu s$) light-induced H^+ release by pR, a negative band at 1742 cm^{-1} appears in the photoproduct absorbance difference spectrum corresponding to the M precursor. This signals the possible presence of L along with K in this pR photoproduct mixture, as well as a perturbation of Glu-108 within the L structure that would be similar to that seen for the homologue residue (Asp-96) in the L state of the bR photocycle. The presence of multiple negative bands assignable to Glu-108 would be a clear indication of heterogeneity in the prephotolysis pR state. The K/L \rightarrow M conversion for pR has an apparent time constant of $50\text{--}70 \mu s$ at room temperature and pH 9.5 in DMPC vesicles. The H^+ donor group in fast H^+ release by pR at pH 9.5 is neither the Schiff base group itself nor its Asp-97 counterion, since H^+ transfer from the former to the latter occurs on a similar time scale as fast H^+ release ($< 100 \mu s$), whereas Asp-97 clearly remains protonated to delay times after photolysis that are at least 50-fold greater than the time required for completion of the fast H^+ release.

Acknowledgment. This work was supported by Syracuse University and by the WM Keck Center for Molecular Electronics.

References and Notes

- (1) Béjà, O.; Aravind, L.; Koonin, E. V.; Suzuki, M. T.; Hadd, H.; Nguyen, L. P.; Jovanovich, S. B.; Gates, C. M.; Feldman, R. A.; Spudich, J. L.; Spudich, E. N.; DeLong, E. F. *Science* **2000**, *289*, 1902–1906.
- (2) Béjà, O.; Spudich, E. N.; Spudich, J. L.; Leclerc, M.; DeLong, E. F. *Nature* **2001**, *411*, 786–789.
- (3) Krebs, R. A.; Dunmire, D. S.; Partha, R.; Braiman, M. S. *J. Phys. Chem. B* **2003**, *107*, 7877–7883.
- (4) Brown, L. S.; Sasaki, J.; Kandori, H.; Maeda, A.; Needleman, R. N.; Lanyi, J. K. *J. Biol. Chem.* **1995**, *270*, 27122–27126.
- (5) Dioumaev, A. K.; Richter, H. T.; Brown, L. S.; Tanio, M.; Tuzi, S.; Saitō, H.; Kimura, Y.; Needleman, R.; Lanyi, J. K. *Biochemistry* **1998**, *37*, 2496–2506.
- (6) Hutson, M. S.; Alexiev, U.; Shilov, S. V.; Wise, K. J.; Braiman, M. S. *Biochemistry* **2000**, *39*, 13189–13200.
- (7) Krebs, R. A.; Alexiev, U.; Partha, R.; DeVita, A. M.; Braiman, M. S. *BMC Physiol.* **2002**, *2*, 5.
- (8) Dioumaev, A. K.; Brown, L. S.; Shih, J.; Spudich, E. N.; Spudich, J. L.; Lanyi, J. K. *Biochemistry* **2002**, *41*, 5348–5358.
- (9) Friedrich, T.; Geibel, S.; Kalmbach, R.; Chizhov, I.; Ataka, K.; Heberle, J.; Engelhard, M.; Bamberg, E. *J. Mol. Biol.* **2002**, *321*, 821–838.
- (10) Varo, G.; Brown, L. S.; Lakatos, M.; Lanyi, J. K. *Biophys. J.* **2003**, *84*, 1202–1207.
- (11) Lakatos, M.; Váró, G. *J. Photochem. Photobiol. B* **2004**, *73*, 177–182.
- (12) Uhmman, W.; Becker, A.; Taran, C.; Siebert, F. *Appl. Spectrosc.* **1991**, *45*, 390–397.
- (13) Braiman, M. S.; Ahl, P. L.; Rothschild, K. J. *Proc. Natl. Acad. Sci. U.S.A.* **1987**, *84*, 5221–5225.
- (14) Gerwert, K.; Souvignier, G.; Hess, B. *Proc. Natl. Acad. Sci. U.S.A.* **1990**, *87*, 9774–9778.
- (15) Hage, W.; Kim, M.; Frei, H.; Mathies, R. *J. Phys. Chem.* **1996**, *100*, 16026–16033.
- (16) Dioumaev, A.; Brown, L. S.; Needleman, R.; Lanyi, J. K. *Biochemistry* **1999**, *38*, 10070–10078.
- (17) Zscherp, C.; Schlessinger, R.; Tittor, J.; Oesterheld, D.; Heberle, J. *Proc. Natl. Acad. Sci. U.S.A.* **1999**, *96*, 5498–5503.
- (18) Xiao, Yaowu; Hutson, M. S.; Belenky, M.; Herzfeld, J.; Braiman, M. S. *Biochemistry* **2004**, *40*, 12809–12818.
- (19) Berge, V.; Amsden, J. J.; Spudich, E. N.; Spudich, J. L.; Rothschild, K. J. *Biochemistry* **2004**, *43*, 9075–9083.
- (20) Aton, B.; Doukas, A. G.; Callender, R. H.; Becher, B.; Ebrey, T. G. *Biochemistry* **1977**, *16*, 2995–2999.
- (21) Dioumaev, A. K.; Wang, J. M.; Balint, Z.; Váró, G.; Lanyi, J. K. *Biochemistry* **2003**, *42*, 6582–6587.
- (22) Sharonov, A. Y.; Tkachenko, N. V.; Savransky, V. V.; Dioumaev, A. K. *J. Photochem. Photobiol.* **1991**, *54*, 889–895.
- (23) Dioumaev, A. K. *Biophys. Chem.* **1997**, *67*, 1–25.
- (24) Roepe, P.; Ahl, P. L.; Das Gupta, S. K.; Herzfeld, J.; Rothschild, K. J. *Biochemistry* **1987**, *26*, 6696–707.
- (25) Gat, Y.; Grossjean, M.; Pinevsky, I.; Takei, H.; Rothman, Z.; Sigrist, H.; Lewis, A.; Sheves, M. *Proc. Natl. Acad. Sci. U.S.A.* **1992**, *89*, 2434–2438.
- (26) Sasaki, J.; Lanyi, J. K.; Needleman, R.; Yoshizawa, T.; Maeda, A. *Biochemistry* **1994**, *33*, 3178–3184.
- (27) Drummond, C. J.; Warr, G. G.; Grieser, F.; Ninham, B. W.; Evans, D. F. *J. Phys. Chem.* **1985**, *89*, 2103–2109.
- (28) Lasch, J.; Berdichevsky, V. R.; Torchilin, V. P.; Koelsch, R.; Kretschmer, K. *Anal. Biochem.* **1983**, *133*, 486–491.
- (29) Sasaki, J.; Yuzawa, T.; Kandori, H.; Maeda, A.; Hamaguchi, H. *Biophys. J.* **1995**, *68*, 2073–2080.
- (30) Kandt, C.; Schlitter, J.; Gerwert, K. *Biophys. J.* **2004**, *86*, 705–717.
- (31) Lakatos, M.; Lanyi, J. K.; Szakacs, J.; Váró, G. *Biophys. J.* **2003**, *84*, 3252–3256.
- (32) Váró, G.; Lanyi, J. K. *Biophys. J.* **1991**, *59*, 313–322.
- (33) Gerwert, K.; Hess, B.; Soppa, J.; Oesterheld, D. *Proc. Natl. Acad. Sci. U.S.A.* **1989**, *86*, 4943–4947.
- (34) Braiman, M. S.; Mogi, T.; Marti, T.; Stern, L. J.; Khorana, H. G.; Rothschild, K. J. *Biochemistry* **1988**, *27*, 8516–8520.
- (35) Imasheva, E. S.; Balashov, S. P.; Wang, J. M.; Dioumaev, A. K.; Lanyi, J. K. *Biochemistry* **2004**, *43*, 1648–1655.
- (36) Althaus, T.; Stockburger, M. *Biochemistry* **1998**, *37*, 2807–2817.
- (37) Heberle, J.; Oesterheld, D.; Dencher, N. A. *EMBO J.* **1993**, *12*, 3721–3727.
- (38) Cao, Y.; Brown, L. S.; Sasaki, J.; Maeda, A.; Needleman, R.; Lanyi, J. K. *Biophys. J.* **1995**, *68*, 1518–1530.
- (39) Lazarova, T.; Sanz, C.; Querol, E.; Padros, E. *Biophys. J.* **2000**, *78*, 2022–2030.
- (40) Sass, H. J.; Büldt, G.; Gessenich, R.; Hehn, D.; Neff, D.; Schlesinger, R.; Berendzen, J.; Ormos, P. *Nature* **2000**, *406*, 649–653.
- (41) Abbreviations: pR, proteorhodopsin; bR, bacteriorhodopsin; Tris, tris(hydroxymethyl)aminomethane; OG, octyl- β -D-glucoside; DMPC, 1,2-dimyristoyl-sn-glycero-3-phosphocholine; TCM, triple cysteine mutant; cmc, critical micelle concentration.